Probing the H^3 vertex in e^+e^-, γe, and $\gamma\gamma$ collisions for light and intermediate Higgs bosons

V. A. Ilyin,* and A. E. Pukhov†
Institute of Nuclear Physics, Moscow State University, 119899 Moscow, Russia

Y. Kurihara‡ and Y. Shimizu§
National Laboratory for High Energy Physics (KEK), Tsukuba, Ibaraki 305, Japan

T. Kaneko‖
Meiji-Gakuin University, Kamikurata, Totsuka 244, Japan
(Received 19 January 1996; revised manuscript received 19 July 1996)

We study double Higgs boson production at future linear colliders while paying special attention to the option of high-energy and high-luminosity photon beams. The main purpose is to examine the feasibility of e^+e^-, γe, and $\gamma\gamma$ colliders in order to establish bounds on the value of triple Higgs coupling, which could be crucial for understanding a spontaneous breaking mechanism. We consider mainly those cases of light and intermediate Higgs bosons, including an analysis of the electroweak backgrounds. The mass range $M_H \sim M_Z$ is discussed separately. It is shown that for a light Higgs boson the H^3 coupling can be visible, even at a future linear e^+e^- collider at 500 GeV. For an intermediate Higgs boson, a collider with TeV energies is suitable for investigations. We estimate the bounds on the anomalous H^3 coupling which can be experimentally established at future linear colliders. [S0556-2821(96)00523-1]

PACS number(s): 14.80.Bn, 12.60.Fr, 14.80.Cp

I. INTRODUCTION

One of the most important problems after future discovery of the scalar boson will be a study of its self-interaction. It will be necessary to clarify the nature of the spontaneous breaking of the gauge symmetry, which provides nonzero masses of intermediate bosons and fermions. In the standard model (SM) one scalar doublet field is introduced:

$$\Phi = \frac{1}{\sqrt{2}} \begin{pmatrix} -\phi_2 - i\phi_1 \\ H + v + i\phi_3 \end{pmatrix}. \tag{1}$$

Here, H is the physical scalar boson (Higgs boson, itself) and the ϕ_i's are unphysical Goldstone fields corresponding to the pure gauge degrees of freedom. The Higgs potential is SU(2) invariant:

$$V(\Phi^*\Phi) = \frac{\lambda_2}{2}(2\Phi^*\Phi - v^2)^2,$$

$$v = \frac{2M_W \sin\theta_W}{e}. \tag{2}$$

Here $e = \sqrt{4\pi\alpha}$ is the electric charge, M_W is the mass of the W boson, and θ_W is the Weinberg mixing angle. The value of the vacuum expectation, $v \approx 250$ GeV, is fixed by parameters of the intermediate bosons obtained from experiments. The coupling constant λ_2 is a free parameter in the SM, and is connected with the Higgs boson mass:

$$\lambda_2 = \frac{\pi\alpha}{4} \frac{M_H^2}{\sin^2\theta_W M_W^2}. \tag{3}$$

The present direct experimental bound on the Higgs boson mass is ~65 GeV [1]. The range $M_H < 105$ GeV (*light* Higgs boson) will be explored by the CERN e^+e^- collider LEP II experiments, while the up-graded Fermilab Tevatron* can scan some heavier masses, up to 120 GeV [2]. The scanning of a higher mass range is expected at the CERN Large Hadron Collider (LHC) (see [3] and the references therein). The observation of a Higgs boson with a mass of up to ~400 GeV (*intermediate* and heavy Higgs bosons) will also be available at future linear colliders with $\sqrt{s} = 500$ GeV, which has been discussed intensively these days [4].

The existence of a relatively light Higgs boson is based on many theoretical models. In supersymmetry (SUSY) extensions of SM (see, for example [5,6] and references therein) several scalar particles are predicted with masses of less than 200 GeV. Grand-unification theories also require such a light Higgs boson in order to provide an experimental value of $\sin^2\theta_W$. Precision tests of the standard model indicate the lightness of a Higgs boson as well [7]. Experiments at LEP II, Tevatron*, LHC, and future linear colliders will crucially expose these intriguing theoretical constructions. Hence, in the situation in which only one scalar boson is discovered, the search for evidence for a nonminimal Higgs boson self-interaction becomes an actual problem. Such evidence could be deviations of the H^3 and H^4 couplings from their SM values, as well as contributions of higher-order vertices (H^n, $n > 4$). Unfortunately, one can easily conclude that the H^4 vertices and higher-order ones are beyond direct experimental probing, even at colliders presently discussed, because of

*Electronic address: ilyin@slava.npi.msu.su
†Electronic address: pukhov@sasha.npi.msu.su
‡Electronic address: kurihara@minami.kek.jp
§Electronic address: shimiz@minami.kek.jp
‖Electronic address: kaneko@minami.kek.jp

the too-small cross sections. Thus, a measurement of the H^3 coupling is the only possibility to test the SM Higgs boson self-interaction and to select new theories.

An anomalous triple Higgs vertex appears in various theoretical constructions. For example, in models with a composite Higgs boson [8] the H^3 coupling can differ from the SM value. Furthermore, we point out the scalar sector in MSSM (minimal supersymmetrical extension of SM) where the triple scalar bosons couplings depend on two free parameters ($\tan\beta$ and $\cot\alpha$) showing up a crucial difference from the Higgs potential of SM (see, e.g., complete set of Feynman rules for MSSM in [9]). Thus, if the mass of the lightest scalar particle is fixed there is still an extra free parameter which contributes to the corresponding triple vertex; also, the measurement of this vertex can be considered to be a possible search for evidence of supersymmetry. Of course, both parameters contribute to other vertices, and one can hope that these parameters will be extracted, for example, from data on superpartners production. Even in this case, a direct measurement of the H^3 coupling will be of great interest due to independent information about the structure of the Higgs sector.

Note that the H^3 vertex contributes to the single Higgs boson production considered as a possible reaction for a Higgs boson discovery *via* next-to-leading loop corrections. However, these corrections should be rather small, while the expected statistical error is on the order of a few percent. It thus seems that this way is closed. Furthermore, although the H^3 coupling is present in tree diagrams on the order of α^n with $n \geqslant 5$ the cross section is also very small due to the higher orders of perturbation theory. As a result, the processes of order of α^3 and α^4 with double Higgs boson production are practically the only opportunity to investigate scalar boson self-interaction.

For trivial kinematical reasons one cannot expect to observe double Higgs boson production at LEP II and Tevatron*, even if the Higgs boson is discovered at these machines. We thus must study prospects of the LHC and future linear colliders in connection with the discussed problem. As for hadron collisions at TeV energies, the relevant calculations are presented in [10–12]. Note that the cross sections in hadron collisions are on the same order as at TeV linear colliders for reactions with the *W-fusion* mechanism of double Higgs boson production. However, much more complicated background conditions which naturally the accompany hadron collisions do not allow any hope to measure the H^3 coupling because of the small cross sections. One could consider a reaction with the *gluon-gluon fusion* mechanism [12], which has larger cross section. However, the gluon-gluon fusion proceeds *via* a t-quark loop, and the sensitivity to H^3 coupling is several times weaker than in the W-fusion reactions (see the corresponding motivation below). We can presumably conclude that hadron collisions have no prospect to resolve the discussed problem.

At the present time the construction of an electron-positron linear collider with a c.m. system (c.m.s.) energy of 500 GeV and with a year-integrated luminosity of 10 fb^{-1} is under discussion, with further extensions up to $\sqrt{s}=2$ TeV and $\mathcal{L}_{\text{year}} \sim 100\ \text{fb}^{-1}$ [4,13,14]. In the text we refer to these two basic steps as $ee500$ and $LC2000$ machines. Several projects are under discussion: the Japan Linear Collider (JLC) (KEK, Japan), TeV Energy Superconducting Linear Collider (TESLA) (DESY, Germany), CERN Linear Collider (CLIC) and Next Linear Collider (NLC) (SLAC). The possibility to realize $e\gamma$ and $\gamma\gamma$ collisions on the basis of the Compton backscattering of laser photons against an electron beam [15,16] is an additional attractive feature of these projects. Thus, three options for future linear colliders are under consideration: e^+e^-, γe, and $\gamma\gamma$. We shall discuss the prospects of all these options in connection with the problem in probing the H^3 coupling.

Backscattered photons generally have a wide energy spectrum. However, if it is possible to shift the interaction point far enough from the conversion one, the low-energy photons will leave the interaction area with relatively large escape angles. In this way a photon beam can be made practically monochromatic, and peaked at a point close to the energy of the basic electron beam $E_\gamma^{\max}$ of $\sim 0.8E_e$. Moreover, when the polarization of the laser photons and that of electrons are opposite, the spectrum of backscattered photons becomes the most monochromatic. It is expected that the luminosity of the $\gamma\gamma$ mode could be on the same order as that for the e^+e^- collider [17–21]. Further, our analysis is based on the cross sections for a monochromatic photon beam. We shall also give the coefficients, which allow one to estimate a convolution with the whole energy spectrum of backscattered photons [15] by rescaling our numerical results.

Another attractive feature of linear colliders is that an electron beam can be highly polarized [22]: 90% of circular polarization is considered to be available using the existing technology. A polarized positron beam has also been proposed [23]: 80% of circular polarization is considered to be realistically achievable. Because of the chirality of electroweak interactions, the use of polarized beams can enhance the cross sections of some processes. This enhancement could be important, because much higher statistics will be needed for some physically interesting processes, and this is a real necessity, e.g., for the discussed double Higgs boson production. We discuss the dependence of the calculated cross sections on the beam polarization.

This paper is organized as follows: In Sec. II an anomalous Higgs potential is introduced. In Sec. III we present the numerical results for some processes and comments on signals with double Higgs boson production. We pay special attention to the case of $M_H \approx M_Z$ in Sec. III D. In Sec. IV we give a detailed analysis of the cross-section dependence on anomalous H^3 coupling for the considered processes in e^+e^-, γe, and $\gamma\gamma$ collisions. We have already presented our preliminary results in [24]. After completing this work we became aware of a similar analysis with calculations made in nonlinear gauge for double Higgs boson production at future linear colliders [25]. Our results are in good agreement if one rescales the fine-structure constant to 1/137 (we used $\alpha=1/128$).

II. ANOMALOUS HIGGS POTENTIAL

To estimate the contribution of the triple Higgs vertex we must change the corresponding constant λ_2 in the Higgs potential (2) while maintaining the SU(2) invariance and the value of the vacuum expectation. We thus add to the SM potential the monomials [26,27]

$$V_n(\Phi^*\Phi)\equiv\frac{\lambda_n}{n!}\,(2\Phi^*\Phi-v^2)^n,\quad n=3,4,\ldots\ . \tag{4}$$

Although many new vertices will appear, only some of them can contribute to the processes on the orders of α^3 and α^4. They are

$$V_3^{(3)+(4)}=\frac{\lambda_3}{6}\,(8v^3H^3+12v^2H^4+12v^2H^2\phi_3^2 + 24v^2H^2\omega^+\omega^-), \tag{5}$$

$$V_4^{(3)+(4)}=\frac{2\lambda_4}{3}\,v^4H^4, \tag{6}$$

where $\omega^{\pm}=(\phi_1\mp i\phi_2)/\sqrt{2}$.

In the unitary gauge, where $\phi_i=0$, this new potential changes only two SM vertices, H^3 and H^4, and results in the appearance of new free parameters, $\lambda_{3,4}$. In other gauges, for example, in renormalizable covariant gauges, all vertices (5) and (6) can contribute, again with two free parameters. Note that the constant at the H^4 vertex remains a free parameter for the processes of $O(\alpha^3)$ and $O(\alpha^4)$. Unfortunately, λ_4 is beyond any experimental study due to the small cross sections of the relevant processes, and only λ_3 coupling can be seen.

We now introduce the dimensionless parameter

$$\delta\equiv\frac{8v^4}{3M_H^2}\,\lambda_3. \tag{7}$$

The value $\delta=0$ implies SM. A nonzero value of the δ parameter can arise in physical models extending SM, e.g., if new physics comes at some scale Λ. This is realized, for example, in composite Higgs models [8], where the constants λ_n of the extended Higgs potential are associated with the corresponding inverse powers of Λ^2, e.g., $|\lambda_3|\sim 1/\Lambda^2$. Of course, the sign of the nonstandard potential terms (4) can be both positive and negative. As we will see, the sensitivity of the discussed processes to the value of anomalous H^3 is different for positive and negative values of δ. Thus, we shall derive two bounds on the *composite* scale $\Lambda^{\pm}$ relatively.

However, such characteristic as the scale Λ is natural for composite models, but not for SUSY models. For example, in MSSM the deviation from SM leads to a violation of the relation (3) between the Higgs boson mass and the triple Higgs coupling constant, even for the lightest scalar boson; here, an extra free parameter appears. Thus, if one would like to discuss the possibility to search for SUSY evidence through the triple Higgs coupling, the consideration of the dimensionless parameter δ is more natural.

It is clear that the cross sections are quadratic in δ:

$$\sigma(\delta)=\kappa(\delta-\delta_{\min})^2+\sigma(\delta_{\min}). \tag{8}$$

Thus, there is some specific point in the corresponding statistical analysis. Let us consider the case when the experiment does not show any deviation from SM at the 95% C.L. for the H^3 coupling. This means that $|N(\delta)-N(0)|<1.96\sqrt{N(0)}$, where $N(\delta)=\mathcal{L}\sigma(\delta)$ is the number of detected events, and $\mathcal{L}$ is the integrated luminosity. Two variants can be realized:

(a) if $\delta_{\min}^2>D^2$ then $\delta^{-+}<\delta<\delta^{--}$ or $\delta^{+-}<\delta<\delta^{++}$,

(b) if $\delta_{\min}^2<D^2$ then $\delta^{-+}<\delta<\delta^{++}$.

Here

$$\delta^{\eta\xi}=\delta_{\min}+\eta\sqrt{\delta_{\min}^2+\xi D^2},$$

$$\eta,\zeta=\pm 1,$$

$$D^2=\frac{1.96\sqrt{\sigma(0)}}{\kappa\sqrt{\mathcal{L}}}.$$

The variant (a) implies that two values of δ correspond to the measured cross section within experimental errors. Furthermore, these two values are separated by fixed interval which does not depend on experimental errors. So we are dealing with some kind of discrete uncertainty which will take place even if a number of measured events corresponds to the level predicted by SM, some *shadow* interval will show up. When the luminosity is small, the variant (b) is realized. However, with increasing the integrated luminosity a discrete uncertainty appears at some critical value ($\hat{\mathcal{L}}$), which depends only on the Higgs boson mass,

$$\hat{\mathcal{L}}=\left(\frac{1.96}{\delta_{\min}^2}\right)^2\frac{\sigma(0)}{\kappa^2}. \tag{9}$$

For the limitations on δ we use two parameters which we denote by $\delta^{\pm}$. In case (b) $\delta^{\pm}=\delta^{\pm+}$. In case (a) they are the bounds of that interval, $(\delta^{-+},\delta^{--})$ or $(\delta^{+-},\delta^{++})$, which includes the SM point $\delta=0$.

Note that by using Eq. (7) one can derive the following formula for the *composite* scales ($\Lambda^{\pm}$) introduced above:

$$\Lambda^{\pm}\sim\frac{10^5\ \mathrm{GeV}^2}{M_H}\,\frac{1}{\sqrt{|\delta^{\pm}|}}.$$

Thus, the bounds established at the level $|\delta^{\pm}|\sim 1$ mean that the composite Higgs boson is excluded at the scale $\Lambda<1$ TeV for $M_H=100$ GeV.

III. CROSS SECTIONS OF DOUBLE HIGGS BOSON PRODUCTION

In this section we present numerical results for the processes with double Higgs boson production. Although we carried out calculations within the framework of the standard model in the 't Hooft–Feynman gauge, we checked some points for each reaction by calculating in the unitary gauge. We used the packages CompHEP [28] and Gran Sasso Air Cherenkov Experiment (GRACE) [31] (see also [32]) for independent calculations of the matrix elements and cross sections. These packages provide automatic tree-level computations of the cross sections and distributions in the standard model and its extensions. Complete set of tree-level diagrams has been generated for each process discussed and coherent summation of these diagrams has been performed. The calculations were made with 1% statistical accuracy, and we checked that both packages gave consistent results. Total cross sections and distributions have been calculated by

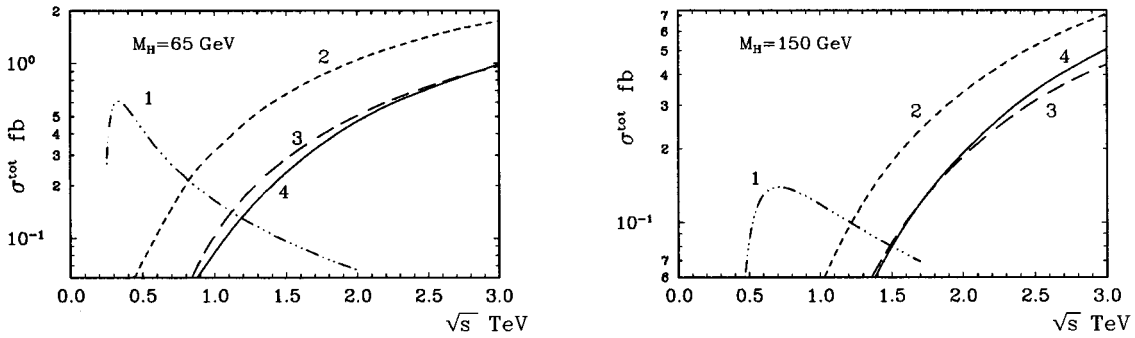

FIG. 1. Energy dependence of the total cross sections of the reactions: (1) $e^+e^-\to ZHH$; (2) $e^+e^-\to\overline{\nu_e}\nu_e HH$; (3) $\gamma e\to\nu_e WHH$; (4) $\gamma\gamma\to W^+W^-HH$.

means of multidimensional Monte Carlo (MC) integration of the matrix element squared. Numerical results were obtained with the following values of the physical constants: $\alpha=1/128$, $M_Z=91.178$ GeV, $\sin\theta_W=0.474$.

In Figs. 1 and 2 we show the dependence of the total cross sections on the energy and M_H for the processes $e^+e^-\to ZHH$, $e^+e^-\to\overline{\nu_e}\nu_e HH$, $\gamma e\to\nu_e WHH$, and $\gamma\gamma\to W^+W^-HH$.

We estimated the number of expected events assuming that all events with double Higgs boson production could be reconstructed from the decay products. Of course this is a very optimistic assumption. We found that in all reactions the angular distribution of Higgs bosons is rather smooth (see some representative histograms in Fig. 3) and the main part of H decay products will be produced at large angles with the beams. So one can hope that efficient reconstruction of double Higgs boson production events is realistic.

When analyzing the signatures in the processes we are discussing one must remember that the light Higgs boson decays into a $b\bar{b}$ pair with a high rate (more than 90%). Thus the main signature of light Higgs boson production is two b-quark jets. However, if $M_H>150$ GeV the Higgs boson decays mainly into WW or ZZ and the signature should be defined by the main modes of W and Z decays, each of them giving dijet in the final state. Although these multijet signatures seem very clean we should note that in the background processes multijets can be produced directly due to multiperipheral mechanisms. Such background processes can have large cross sections in the presence of QCD coupling, creating difficulties for the signal separation especially in $\gamma\gamma$ collisions. Reliable separation of this background is a difficult calculation problem, and we need here in not only advanced calculation techniques. Below we discuss some specific features of distributions in the processes under consideration which can allow one to apply suitable cuts in order to suppress direct multijet background.

A. e^+e^- collisions

(a) $e^+e^-\to ZHH$. In this process the Higgs particles are produced by the H bremsstrahlung from the Z boson line. This process was discussed in [29,11], and we have only confirmed those numerical results. The cross section has a maximum and decreases with energy far enough from the threshold $\sqrt{s}=2M_H+M_Z$. For a light Higgs boson the cross section maximum is located rather close to the energy expected for the $ee500$ collider.

This reaction has no competitive electroweak background; for $M_H<150$ GeV the main signature is $Zbbbb$, giving a six-jet final state in the case of hadronic decays; for $M_H>150$ GeV the signature, $ZWWWW$, gives up to 10 jets.

We might hope that in the case of light Higgs boson the observation of more than five events per year is plausible at the $ee500$ collider. Note that the often-discussed initial-state radiation reduces the total cross section by less than 7%. We should also mention that the rate of this reaction might increase by a factor of up to 2 when electrons and positrons are

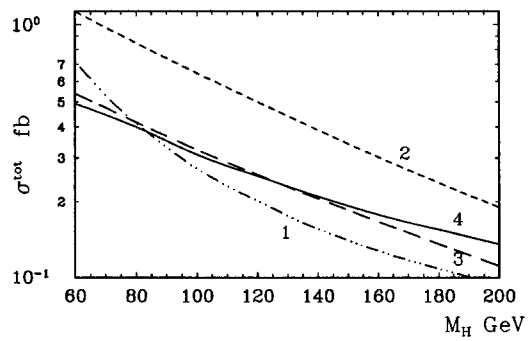

FIG. 2. Total cross section vs the Higgs boson mass for the same processes as in Fig. 1. For $e^+e^-\to ZHH$, $\sigma^{\rm tot}$ is calculated at energies corresponding to its maxima. For other processes the curves were calculated at $s=2$ TeV.

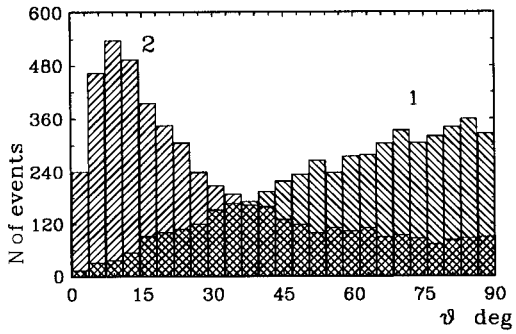

FIG. 3. Higgs boson angular distributions in the reactions: (1) $e^+e^-\to ZHH$ at $M_H=65$ GeV and $\sqrt{s}=335$ GeV; (2) $e^+e^-\to\overline{\nu_e}\nu_e HH$ at $M_H=150$ GeV, and $\sqrt{s}=2$ TeV. For each distribution 5000 events were generated.

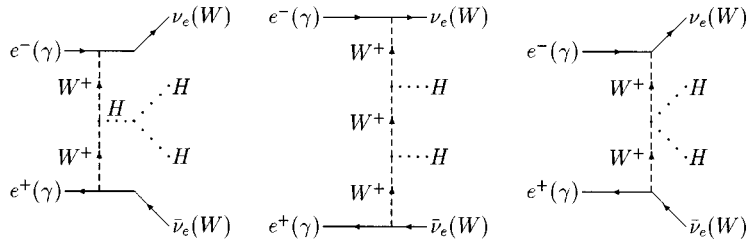

FIG. 4. Feynman diagrams of the fusion mechanism $W^+W^- \to HH$. For the discussed processes the virtual incoming W bosons are suspended from the initial electron (positron) or photon.

polarized, due to the conservation of fermion chirality in the *Z-fermion-fermion* vertex.

(b) $e^+e^- \to \overline{\nu_e}\nu_e HH$. This process has been discussed in [30]. Our numerical results are in agreement with this paper. In this reaction the diagrams with *W-fusion* (see Fig. 4) give the main contribution to the cross section. Due to the contribution of these diagrams with a vector boson exchange in the t channel, the total cross section increases with energy (see Fig. 1). The cross section is small enough at the energy of the $ee500$ collider showing no practical interest to search for double Higgs boson events. However, the cross section increases rather rapidly and already at 1.5 TeV a real opportunity appears. This reaction has the biggest cross section among other double Higgs boson production processes.

The final states are identified by Higgs boson decay. The main signature for $M_H < 150$ GeV is four jets. For larger Higgs boson masses it is four gauge bosons ($WWWW$, $WWZZ$,$ZZZZ$) with their subsequent decays, giving up to eight jets. The possible electroweak background could be given by the reaction $e^+e^- \to HH$, where the H^3 vertex gives a negligible contribution because it is accompanied by the *H-electron-electron* vertex. Nevertheless, on the one-loop level this reaction has a relatively large cross section due to the contributions of other vertices (see Table I), and should be considered as background. However, one can see from Fig. 5 that the missing energy is large (about 80% of the total energy) in the reaction $e^+e^- \to \overline{\nu_e}\nu_e HH$, thus one can hope that the corresponding criteria for the event selection will help a great deal for the separation from the double Higgs boson events produced in the reaction $e^+e^- \to HH$.

As we will see below, all processes with double Higgs boson production through the W-fusion mechanism are characterized by explicit energy separation of the spectators (neutrinos or W bosons) from the Higgs bosons, typical histograms we give in Fig. 5. Surely, this effect should help also in the separation of the signal from the direct QCD multijet background. Furthermore we found that the spectators in the processes with W-fusion mechanism have large transverse momentum, at least $p_t > 10$ GeV/c for the $LC2000$ collider. So the large p_t of the spectators is caused by the exchange of massive W bosons, in the t channel (see diagrams in Fig. 4). One can hope that the large p_t of decay products of W bosons (if they are detected) or large missing p_t (due to invisible neutrino or undetectable W bosons) could help us to separate the HH signal.

Since only the left-handed electron and the right-handed positron contribute to this reaction, the statistics increase by a factor of 3–4 if the electron and positron beams are polarized. For unpolarized experiments 34 events per year will be observed for $M_H = 150$ GeV at $LC2000$. Note that for the reaction $e^+e^- \to \overline{\nu_e}\nu_e HH$ the initial-state radiation reduces the cross section more seriously (by $\sim 20\%$) than for the $e^+e^- \to ZHH$ reaction.

(c) Other processes with double Higgs boson production in e^+e^- collisions have cross sections that are too small (see Table I) to be of practical interest, even at $LC2000$. We only note that the reaction $e^+e^- \to ZHHH$ could be of particular interest because it is the only one where the H^4 vertex contributes.

TABLE I. Unpolarized cross sections of different channels in e^+e^- collisions with double and triple Higgs boson production. These calculations were performed in the standard model with Higgs boson mass $M_H = 65$ GeV. The values of $s_{\max}$ correspond to energies where cross sections reach their maxima.

e^+e^- channel	$\sqrt{s}$	σ^{tot} (fb)
ZHH	$\sqrt{s}_{\max} = 335$ GeV	0.61
$\overline{\nu_e}\nu_e HH$	2 TeV	1.0
e^+e^-HH	2 TeV	0.13
HH [33]	>250 GeV	<0.1
$\overline{tt}HH$	$\sqrt{s}_{\max} = 800$ GeV	0.063
W^+W^-HH	$\sqrt{s}_{\max} = 700$ GeV	0.035
$ZZHH$	$\sqrt{s}_{\max} = 610$ GeV	0.0043
$ZHHH$	$\sqrt{s}_{\max} = 520$ GeV	0.8×10^{-3}

B. γe collisions

(a) $\gamma e \to \nu_e WHH$. In this reaction the Higgs bosons are produced by means of the W-fusion mechanism (Fig. 4), similarly to the $e^+e^- \to \overline{\nu_e}\nu_e HH$ case. In total 13 generic Feynman diagrams contribute, each of them producing a number of additional diagrams with ϕ_i fields, see Eq. (1),

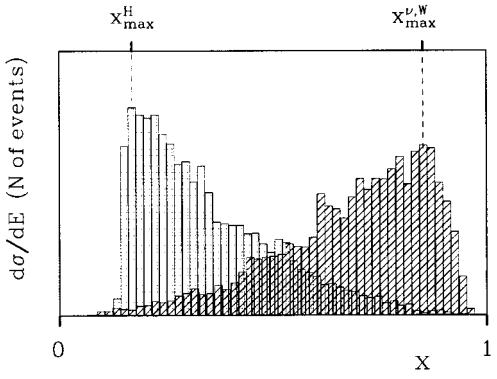

FIG. 5. Energy distribution of outgoing particles in reactions involving the W-fusion mechanism. Here, $x \equiv 2E/\sqrt{s}$. For the Higgs bosons $x_{\max} < (M_H + M_W)/\sqrt{s}$. For spectators ($\nu_e$ or W bosons) $x_{\max} \sim 1 - 2(M_H + M_W)/\sqrt{s}$. This picture is typical for $\sqrt{s} \sim 2$ TeV and $M_H = 100$–300 GeV.

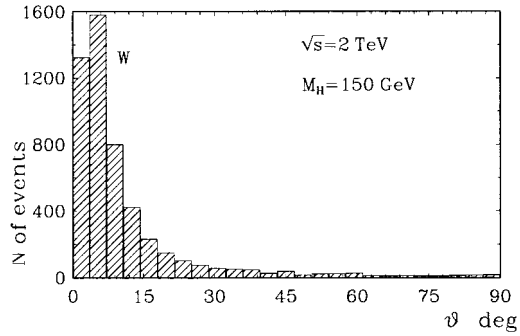

FIG. 6. Angular distribution of W in $\gamma\gamma\to W^+W^-HH$; 5000 events have been generated.

Goldstone partners of W and Z bosons. The cross section increases with energy and at 2 TeV reaches the order of tenths of fb showing a real possibility to study the H^3 coupling.

The W boson is emitted mainly in the direction close to the photon beam within 2°–3° cone around the γ beam direction (the W angular distribution in the process is similar to the W angular distribution in the $\gamma\gamma\to W^+W^-HH$ reaction (see Fig. 6). The W boson energy is the order $(\sqrt{s}/2-M_H-M_W)$ (see Fig. 5) and it easy to show that about 90% of the events will have W decay products going into the forward 5° cone, and more than 50% going to the forward 2° cone. We conclude that the event selection has to include the following criteria: (1) two high-energy jets with the invariant mass peaking at M_W; (2) large missing energy.

About 20 events per year can be observed for $M_H=150$ GeV at $LC2000$. The convolution with the photon spectrum decreases the cross section by three times for $M_H<300$ GeV and $\sqrt{s}\sim 2$ TeV. Since only the left-handed electrons contribute to this reaction, its cross section increases with the rate of the electron-beam longitudinal polarization, while the dependence on the photon polarization is less than 3% at $\sqrt{s}\sim 1$–2 TeV.

(b) $\gamma e\to eZHH$. The total cross section decreases with the energy and Higgs boson mass. For $M_H=65$ GeV the maximum is $\sigma^{\rm tot}_{\rm max}=0.009$ fb at $\sqrt{s}\approx 500$ GeV; this reaction has very small total cross section and is beyond any experimental study.

C. $\gamma\gamma$ collisions

In $\gamma\gamma$ collisions double Higgs boson production can occur in several reactions at the tree level and in one process, $\gamma\gamma\to HH$, at the one-loop level. All of these processes are of the order α^4.

(a) $\gamma\gamma\to W^+W^-HH$. At high energies the Higgs bosons are produced in this reaction again with the help of W-fusion mechanism (see Fig. 4, in total 49 generic Feynman diagrams contribute). So the total cross section increases with energy. We also note that it decreases with the Higgs boson mass more slowly than in the γe reaction, and already for $M_H>120$ GeV $\gamma\gamma$ reaction gives more double H events (Fig. 2).

As in $\gamma e\to\nu_e WHH$ reaction the W bosons escape closely to the collision axis, concentrating at the angles of the order 3°–4° (see Fig. 6). Again we conclude that due to the large energy of W bosons (see Fig. 5) about 90% of the events will have W decay products going into forward or backward 5° cones. If the detection of particles is not easy at such small angles, the triggering must include a large missing energy. One should note that the reaction $\gamma\gamma\to HH$ will give a background comparable with the signal only if the Higgs boson decay products are detected without any missing energy.

Our conclusion is that for light and intermediate Higgs bosons a noticeable number of events will be produced. For example, for $M_H=150$ GeV about 20 events can be seen per year at $LC2000$ and about 14 events can be observed for $M_H=200$ GeV.

The convolution with the whole photon spectrum decreases the cross section by 7–12 times for $M_H=100$–200 GeV. The dependence on the photon polarization is only within 7% at $\sqrt{s}\sim 2$ TeV.

(b) $\gamma\gamma\to ffHH$, where f is a fermion. Since the *H-fermion-fermion* coupling is proportional to the fermion mass, we calculated only the t-quark case to estimate the upper bound of the cross sections. The total cross section decreases with the energy and Higgs boson mass; for $M_H=65$ GeV it has a maximum value of 0.07 fb at $\sqrt{s}=850$ GeV and $m_{\rm top}=170$ GeV. Hence, this reaction can have visible statistics only for light Higgs boson and the integrated luminosity higher than 100 fb^{-1}.

(c) $\gamma\gamma\to HH$. This reaction proceeds at the one-loop level. Analytical formulas for the amplitudes and a detailed numerical analysis are presented in [34,35]. The rate of this reaction is comparable with that of the $\gamma\gamma\to W^+W^-HH$ process at $M_H<300$ GeV and $\sqrt{s}>1$ TeV. These two reactions have comparable cross sections in the case when no W decay products are detected. Of course, a large missing energy, occurring in the W-fusion reaction, would help to separate the events of these two channels.

D. Case of $M_H\approx M_Z$

When M_H is close to the Z boson mass it is difficult to separate the signal from the Z background by reconstructing the *jet-jet* mass. A b-tagging procedure can be used to separate the signal in this case. This procedure is based on searching for a second vertex from the b decay by a high-resolution vertex detector. We collect in Table II the total cross sections of double Higgs reactions together with those of the background processes. In the same table we give the estimates of the *signal-to-background* ratio (S/B) calculated by two methods.

(I) The ratio is calculated by the method proposed in [36]. It is realistic to assume a 80% b-tagging efficiency. At this efficiency misidentification of b quark as light quark can be taken to be equal to 0.5%, while for the c quark it is 35%. At least two b quarks are assumed to be tagged for separating the HH signal.

(II) The ratio is also calculated by applying the highest efficiency for b-tagging when the value of the S/B ratio is given by

$$\frac{\sigma_{\rm signal}}{\sigma^{ZZ}_{\rm bg}\cdot B(Z\to b\bar{b})^2+\sigma^{ZH}_{\rm bg}\cdot B(Z\to b\bar{b})}, \tag{10}$$

which is the most optimistic estimate.

To determine the possibility of separating the signal com-

TABLE II. Unpolarized total cross sections of signal and background processes at the point $M_H=M_Z$. The signal/background ratio was estimated in two ways: (I) with a realistic assumption concerning the b-tagging efficiency and quark contamination [36], (II) with the formula (10) based on a direct account of the $Z\to bb$ branching.

Case of $M_H=M_Z$				
Signal reactions and backgrounds	$\sqrt{s}$ (TeV)	$\sigma^{\rm tot}$ (fb)	S/B (I)	S/B (II)
$e^+e^-\to ZHH$	0.5	0.31	0.56	
ZZZ		1.15		
ZZH		0.95		
$e^+e^-\to\overline{\nu_e}\nu_eHH$	2	0.73	0.13	0.42
$\overline{\nu_e}\nu_eZZ$		33.8		
$\overline{\nu_e}\nu_eZH$		6.48		
$ee\to e^+e^-ZZ$		4.65		
e^+e^-ZH		1.20		
$\gamma e\to\nu_eWHH$	2	0.36	0.12	0.26
ν_eWZZ		31.1		
ν_eWZH		4.49		
$\gamma\gamma\to W^+W^-HH$	2	0.34	0.06	0.14
W^+W^-ZZ [37]		65.6		
W^+W^-ZH		6.35		

ing from the $e^+e^-\to ZHH$ process, we must use a hadronic decay mode of the Z boson. In this case the signal is six jets with four b-quark jets from two H decays. One can see from Table II that after b-tagging a ratio (S/B) of $\sim$0.56 can be achieved. This value allows us to hope that a number of HH events will be identified at the $ee500$ collider. Unfortunately, even with this value one cannot hope to measure the H^3 coupling in the realistic experiment.

For W-fusion reactions the situation is much worse, and we cannot hope to separate any noticeable number of events with double Higgs boson production. For the reactions $e^+e^-\to\overline{\nu_e}\nu_eHH$ and $\gamma e\to\nu_eWHH$, after b-tagging one can expect the S/B ratio to be at the very small level $\sim$0.13. Even if we apply the most optimistic estimate of type II, the S/B ratio is not larger than 0.3–0.4. Also note that for the e^+e^- reaction another type of background could arise from the $e^+e^-\to e^+e^-Z\mathcal{B}$ processes, where $\mathcal{B}$ denotes Z or H, with electrons and positrons being hidden in the forward-backward invisible cones, or when they escape with too small energies. Indeed, the corresponding total cross sections are relatively large (see Table II). However, if we veto the electrons and positrons to be observed in a visible region and apply the missing momentum cut at for instance several tens of GeV, this background can be reduced to less than 1/1000 with keeping almost all signal events.

For the reaction $\gamma\gamma\to W^+W^-HH$ the situation is more complicated because of the larger value of the background cross sections (see Table II), and one can expect the S/B ratio to be not larger than 0.1.

Probably, another method to separate H and Z events by using the angular distributions of their decay products [38] could help. However, since this method also discards signal events, we need higher luminosity colliders.

IV. δ SENSITIVITY

In this section we analyze numerically the sensitivity of cross sections to the anomalous H^3 coupling. The representative parameters characterizing this sensitivity are collected in Table III (see Sec. II for definitions). In this table you find cross sections of processes under consideration calculated at three values of anomalous H^3 coupling, $\delta=0,\pm1$. We remind the reader that dimensional parameter δ represents the anomalous triple Higgs coupling λ_3, Eqs. (4) and (7). These numerical results give an opportunity to reconstruct parameters of quadratic function (8), we give in Fig. 7 representative curves for process $\gamma\gamma\to W^+W^-HH$ for some values of Higgs boson mass. The last two columns represent the interval (δ^-,δ^+) which characterizes the sensitivity at integrated luminosity $\mathcal{L}$ of 100 fb^{-1}. If δ lies on the interval (δ^-,δ^+) the deviation from the SM cannot be registered within statistical error, so the wider the interval is, the less the sensitivity is.

We found that for Higgs boson mass range under discussion and integrated luminosities of future linear colliders (10–100 fb^{-1}) the cross sections are expected to be close to the minimum point of quadratic function (8) (see also Fig. 7). As a result, when integrated luminosity is higher than parameter $\hat{\mathcal{L}}$, Eq. (9), the effect of discrete uncertainty does manifest. It means that two different intervals (δ^-,δ^+) and a *shadow* one (see Sec. II), exist where the cross section has the same value as predicted by the SM within statistical errors. If the integrated luminosity is close to $\hat{\mathcal{L}}$ or lower, these two intervals join and, as a result, the sensitivity to δ gets drastically weaker.

We discuss below some further features of the δ sensitivity in the cases of light, intermediate, and heavy Higgs bosons.

Light Higgs boson. As noted above, only the process $e^+e^-\to ZHH$ gives some prospects to be examined at the $ee500$ collider due to its rather large cross section. The effect of the *shadow* interval is present at the integrated luminosity of 10 fb^{-1}. Since the two intervals are very close to each other (see Table IV) the real bounds are rather weak: $-10<\delta<2$.

At $LC2000$ a much stronger δ limitation can be established in W-fusion reactions, see Table III, especially for the reaction $e^+e^-\to\overline{\nu_e}\nu_eHH$.

In the e^+e^- reaction the effect of a discrete uncertainty shows up rather clearly (see Table IV), and the corresponding shadow interval could be resolved in the $\gamma\gamma$ mode of $LC2000$, thus demonstrating the complementarity of different options of planned linear colliders. Combined data from

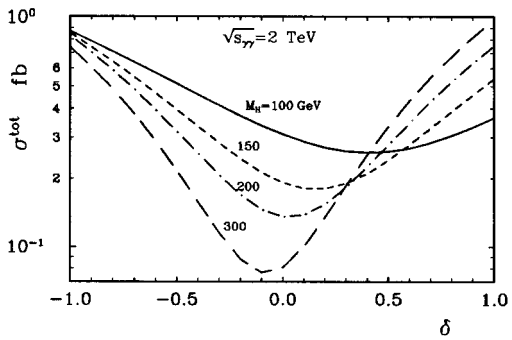

FIG. 7. Total cross-section dependence on the H^3 anomalous coupling δ for $\gamma\gamma\to W^+W^-HH$.

TABLE III. Unpolarized total cross sections and parameters representing the dependence on the anomalous H^3 coupling δ. For the γ channels the results are obtained for monochromatic photon beam(s). The values of the cross section for the $e^+e^-\to ZHH$ reaction are given at points of its maxima (the corresponding energies in TeV are indicated in brackets). For other processes the cross sections were calculated at $\sqrt{s}=2$ TeV. Parameters $\delta^{\pm}$ are limitations on δ available at an integrated luminosity of 100 fb^{-1}. Parameter $\hat{\mathcal{L}}$ matches the Higgs boson masses for which the shadow interval exists; it appears in addition to the limitation interval, $\delta^-<\delta<\delta^+$, if the integrated luminosity is higher than $\hat{\mathcal{L}}$.

Process	M_H (GeV)	Cross sections (pb) $\delta=0$ (SM)	$\delta=-1$	$\delta=1$	$\hat{\mathcal{L}}$ (fb^{-1})	δ^-	δ^+
$e^+e^-\to ZHH$	65	0.61 (0.335)	0.41	0.87	9	−0.73	0.62
	M_Z	0.32 (0.44)	0.20	0.49	21	−0.88	0.69
	120	0.20 (0.56)	0.12	0.32	36	−1.1	0.77
	150	0.14 (0.7)	0.079	0.23	58	−1.3	0.82
	200	0.094 (0.95)	0.050	0.17	109	−4.8	0.85
	250	0.072 (1.2)	0.036	0.13	143	−4.4	0.86
	300	0.059(1.5)	0.029	0.12	180	−4.1	0.85
$e^+e^-\to\overline{\nu_e}\nu_e HH$	65	1.0	1.6	0.77	42	−0.42	0.61
	M_Z	0.73	1.4	0.52	64	−0.34	0.55
	120	0.49	1.2	0.41	133	−0.30	1.6
	150	0.34	0.99	0.37	262	−0.28	1.2
	200	0.19	0.81	0.40	1116	−0.27	0.77
	250	0.11	0.67	0.41	4871	−0.27	0.56
	300	0.066	0.55	0.41	$>10^4$	−0.27	0.44
$\gamma e\to\nu_e WHH$	65	0.51	0.86	0.37	100	−0.47	2.8
	M_Z	0.36	0.78	0.28	169	−0.38	1.8
	120	0.26	0.71	0.27	381	−0.33	1.3
	150	0.19	0.65	0.31	1088	−0.32	0.91
	200	0.11	0.58	0.38	$>10^4$	−0.31	0.58
	250	0.072	0.51	0.44	$>10^4$	−0.32	0.41
	300	0.048	0.45	0.45	$>10^4$	−0.33	0.33
$\gamma\to W^+W^-HH$	65	0.46	0.86	0.38	213	−0.43	1.9
	M_Z	0.34	0.86	0.36	370	−0.34	1.3
	120	0.25	0.86	0.43	1102	−0.30	0.85
	150	0.20	0.86	0.55	5817	−0.29	0.59
	200	0.13	0.84	0.76	$>10^4$	−0.30	0.36
	250	0.10	0.80	0.92	$>10^4$	−0.33	0.25
	300	0.08	0.75	0.99	$>10^4$	−0.35	0.20
	500	0.033	0.36	0.61	1641	−0.45	0.17

the two experiments could establish the limitation at the level of $-0.4<\delta<0.6$ without the shadow interval.

Intermediate Higgs boson. First, one can see that the $ee500$ collider has no feasibility for these Higgs boson masses in all W-fusion processes due to the too-small cross sections (see Fig. 1). However, for a small interval, $M_Z<M_H<100$ GeV, some weak limitations still can be established in the reaction $e^+e^-\to ZHH$, see Table IV.

For $LC2000$ the situation is much better. We note that the lower bound does not practically depend on the reaction. Furthermore this lower bound does not depend on the value of Higgs boson mass, within the rather wide interval from 100 to 300 GeV. As for the upper bound δ^+ the reaction $e^+e^-\to\overline{\nu_e}\nu_e WW$ is better for $M_H<110$ GeV. However, for larger masses, $M_H>120$ GeV, the $\gamma\gamma$ reaction gives the best chance to establish limitations on δ.

For the intermediate Higgs boson the effect of the shadow interval appears in the analysis of the $e^+e^-\to\overline{\nu_e}\nu_e WW$ reaction for $M_H<110$ GeV at the integrated luminosity of 100 fb^{-1}. Again we note, that the $\gamma\gamma$ mode of $LC2000$ can resolve this shadow interval, see the Table IV.

We would like also to note that if the $\gamma\gamma$ luminosity can be increased significantly (for example, as discussed in [18,21]), the $\gamma\gamma$ reaction can set extremely strict limitations on δ. In the case of $\mathcal{L}\sim10^4$ fb^{-1} (probably too optimistic) these bounds can be established at the $-0.05<\delta<0.08$ level together with the shadow interval of $0.2<\delta<0.35$.

Heavy Higgs boson. For Higgs boson masses of hundreds GeV we found an interesting effect of a large enhancement of the total cross sections of W-fusion reactions for large values of the anomalous coupling δ. We show some representative curves for three values of H^3 anomalous coupling in Fig. 8. This effect can be explained by the competition of two factors. One factor is associated with a decrease of the total phase space due to large Higgs boson masses. The other one is specific for the processes under investigation, and is

TABLE IV. Prospects to establish bounds on the triple Higgs coupling at future linear colliders.

M_H (GeV)	Collider	Best channel	(δ^-,δ^+)	Shadow interval	Composite scale (TeV)
70–85	$ee500$	$e^+e^-\to ZHH$	$(-4,2)$	$(-10.2,-4.4)$	-
70–85	$LC2000$	$e^+e^-\to\overline{\nu_e}\nu_eHH$	$(-0.4,0.6)$	(2,5,3.5)	From both reactions,
		$\gamma\to W^+W^-HH$	(0.4,1.8)	-	at $M_H=80$ GeV:
					$\Lambda^+\approx1.6$, $\Lambda^-\approx2.0$
95–100	$ee500$	$e^+e^-\to ZHH$	$(-8,2)$	-	-
95–110	$LC2000$	$e^+e^-\to\overline{\nu_e}\nu_eHH$	$(-0.3,0.6)$	(1.3,2.2)	From both reactions,
		$\gamma\gamma\to W^+W^-HH$	$(-0.3,1.0)$	-	at $M_H=100$ GeV:
					$\Lambda^+\approx1.3$, $\Lambda^-\approx1.8$
110–200	$LC2000$	$\gamma\gamma\to W^+W^-HH$	$(-0.3,0.9$–$0.36)$	-	$\Lambda^+\approx1.0$–0.8
					$\Lambda^-\approx1.7$–0.9
<700	$LC2000$	W-fusion	$\lvert\delta\rvert\sim1$ can be detected		-
>700	$LC2000$	$\gamma\gamma\to HH$ [35]	bounds at the level $\delta\sim1$		-

associated with an increase of that part of the phase space where the Higgs boson propagator can be considered as a constant (when the corresponding squared momentum can be neglected in comparison with M_H). For a larger δ the second factor becomes significant, because the H^3 vertex is accompanied by the Higgs boson propagator, see the first (signal) diagram in Fig. 4. Thanks to this effect the anomalous H^3 coupling in the W-fusion processes becomes detectable for rather large masses. For example, the value $|\delta|=1$ can be measured up to $M_H=700$ GeV at LC2000.

We now give some conclusions concerning the reaction $\gamma\gamma\to HH$ using the results from [35]. The important point is that the anomalous H^3 coupling contributes only to amplitudes with equal photon helicities. However, for such photon polarizations and for $M_H<300$ GeV the cross section is dominated by diagrams with a t-quark loop: $\sim100\%$ for $\sqrt{s}>1$ TeV. Consequently, the origin of the δ dependence in this reaction is different from W-fusion reactions. As a result, the sensitivity to δ is several times weaker here. For example, from the figures presented in [35] one can pick out the following cross sections for $M_H=250$ GeV: $\sigma^{\rm tot}(\delta=0)\sim0.104$ fb, $\sigma^{\rm tot}(-1)\sim0.112$ fb and $\sigma^{\rm tot}(1)\sim0.1$ fb. Hence, the possible limitation is $-4.3<\delta<7.3$. Such a weak sensitivity means that the interaction of the Higgs boson with W boson has a stronger dependence on the anomalous H^3 coupling than the interaction with fermions does. Certainly, this difference is associated with the fact that the *Higgs-W* interaction is deeply involved in the mechanism of the spontaneous breaking of the local gauge invariance. One can find a supporting argument in some other figures presented in [35]. In fact, for $M_H>500$ GeV and $\sqrt{s}>1$ TeV the main contribution to the amplitudes with equal photon polarizations comes from the W-loop diagrams; in this mass range the sensitivity to δ increases significantly.

V. CONCLUSIONS

The main conclusion is that the H^3 vertex can be studied in W-fusion reactions ($e^+e^-\to\overline{\nu_e}\nu_eHH$, $\gamma e\to\nu_eWHH$, and $\gamma\gamma\to W^+W^-HH$) at 2 TeV linear colliders with an integrated luminosity of 100 fb^{-1}. We point out the following important aspects.

All modes of the linear collider (e^+e^-, γe, and $\gamma\gamma$) can be used for probing the H^3 coupling.

Because of poor statistics it will be necessary to accumulate all events with double Higgs boson production. After several years of operating the limitation at the level of $|\delta|<0.5$ (coming from W-fusion reactions) is realistic for the Higgs boson with mass less than 300 GeV.

The rates of double Higgs boson production could be greatly increased if the colliding electron and positron beams are polarized. The polarization of photon beam does not noticeably affect the cross sections.

The signatures of the processes discussed are clear (several jets, up to 8–12, with invariant masses peaked at M_H and M_W) without any electroweak background. Various fea-

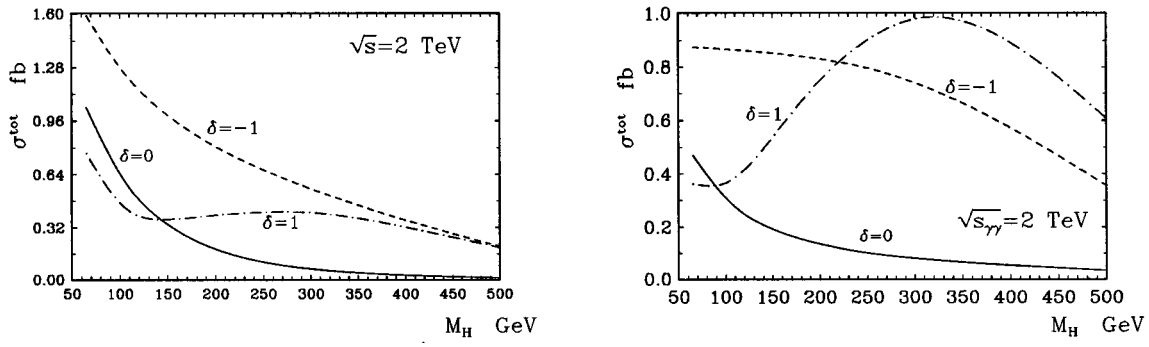

FIG. 8. Total cross section vs the Higgs boson mass for large values of the anomalous H^3 coupling constant: left-hand side for $e^+e^-\to\overline{\nu_e}\nu_eHH$; right-hand side for $\gamma\gamma\to W^+W^-HH$.

tures (such as a large missing p_t and energy, energy separation of Higgs boson decay products and spectators) could be used to suppress direct multijet background.

In the case of e^+e^- reactions the statistical analysis gives two limitation intervals of δ for the *light* and *intermediate* Higgs bosons: the interval around the SM value together with *shadow* one. Such a discrete uncertainty might be resolved with the help of the $\gamma\gamma$ reaction, what shows a complementarity of the different modes of future linear colliders.

Anomalous $\delta=\pm 1$ couplings are available to be detected for Higgs boson masses up to several hundred GeV in W-fusion reactions.

For very heavy Higgs boson, $M_H>700$ GeV, only the reaction $\gamma\gamma\to HH$ can be used for study of the H^3 coupling.

Some observation could be made at the $ee500$ collider in the $e^+e^-\to ZHH$ reaction for a light Higgs boson.

Finally we note that the range $M_H\sim M_Z$ is not good for probing the H^3 coupling in any reactions due to the identity of two jet signals from the Higgs and Z bosons. In this case, even the b-tagging will not help due to the large cross sections of the background processes.

ACKNOWLEDGMENTS

This work was supported in part by the Japan Society for the Promotion of Science. V.A.I. and A.E.P. were also partially supported also by the European association INTAS (Project No. 93-1180) and the Grant Center for Natural Sciences of State Committee for Higher Education in Russia (Grant No. 95-0-6.4-38). We are also indebted to KASUMI Co. Ltd. and SECOM Co. Ltd. for financial support to our collaboration. V.A.I. and A.E.P. are grateful to M. N. Dubinin and V. I. Savrin for many discussions. V.A.I. expresses his deep gratitude to the Minami-Tateya collaboration (KEK) for both hospitality and providing him with excellent conditions to stay and work in Japan.

[1] M. Pohl, in *Proceedings of the 27th International Conference on High Energy Physics*, Glasgow, Scotland, 1994, edited by P. J. Bussey and I. G. Knowls (IOP, London, 1995), p. 107.

[2] A. Belyaev, E. Boos, and L. Dudko, Mod. Phys. Lett. A **10**, 25 (1995).

[3] M. Spira *et al.*, Nucl. Phys. **B453**, 17 (1995).

[4] See, e.g., Nucl. Instrum. Methods Phys. Res. A **355**, (1995); *Proceedings of the 2nd Workshop on Physics and Experiments with Linear e^+e^- Colliders*, Waikoloa, Hawaii, 1993, edited by F. A. Harris *et al.* (World Scientific, Singapore, 1993); *e^+e^- Collisions at 500 GeV: The Physics Potential*, Proceedings of the Workshop, Munich, Annecy, Hamburg, 1991, edited by P. W. Zerwas (DESY Report No. 92-123A,B,C, Hamburg, 1993); ''JLC-I,'' KEK Report No. 92-16, 1992 (unpublished).

[5] J. F. Gunion, H. E. Haber, G. Kane, and S. Dawson, *The Higgs Hunter's Guide* (Addison-Wesley, Reading, MA, 1990).

[6] A. Djouadi, J. Kalinowski, and P. W. Zerwas, in *e^+e^- Collisions at 500 GeV: The Physics Potential* [4], p. 83.

[7] J. Ellis, G. L. Fogli, and E. Lisi, Z. Phys. C **69**, 627 (1996); P. Langacker, National Science Foundation Report No. NSF-ITP-95-140, UPR-0683T, 1995 (unpublished).

[8] D. B. Kaplan and H. Georgi, Phys. Lett. **136B**, 183 (1984); H. Georgi, *ibid.* **151B**, 57 (1985); Yu. F. Pirogov, Int. J. Mod. Phys. A **7**, 6473 (1992); Mod. Phys. Lett. A **8**, 3129 (1993).

[9] J. Rosiek, Phys. Rev. D **41**, 3464 (1990).

[10] O. J. P. Éboli *et al.*, Phys. Lett. B **197**, 269 (1987); W.-Y. Keung, Mod. Phys. Lett. A **2**, 765 (1987); K. J. Kallianpur, Phys. Lett. B **215**, 392 (1988); D. A. Dicus, C. Kao, and S. S. D. Willenbrock, *ibid.* Phys. Lett. B **200**, 187 (1988).

[11] V. Barger, T. Han, and R. J. N. Philips, Phys. Rev. D **38**, 2766 (1988).

[12] D. A. Dicus, C. Kao, and S. S. D. Willenbrock, Phys. Lett. B **203**, 457 (1988); E. W. N. Glover and J. J. van der Bij, Nucl. Phys. **B309**, 282 (1988).

[13] Proceedings of the 2nd European Workshop on Physics with e^+e^- Linear Colliders, Assergi, Gran Sasso, Italy, 1995 (unpublished).

[14] Proceedings of the 3rd Workshop on Physics and Experiments with Linear e^+e^- Colliders, LCWS95, Morioka-Appi, 1995 (World Scientific, Singapore, 1996).

[15] I. F. Ginzburg *et al.*, Pis'ma Zh. Eksp. Teor. Fiz. **34**, 514 (1981) [JETP Lett. **34**, 491 (1981)]; Nucl. Instrum. Methods **205**, 47 (1983); I. F. Ginzburg *et al.*, *ibid.* **219**, 5 (1984).

[16] E. L. Saldin *et al.*, DESY Report No. 94-243, 1994 (unpublished).

[17] We are grateful to I. F. Ginzburg for discussion of this point. The corresponding references are [15,18,19]. Recent discussion has led to conclusion [20,14] that the $\gamma\gamma$ luminosity can be 1/2–1/5 of the luminosity of basic e^+e^- collider with practically monochromatic photon beam. We refer also to [18,21] where an idea to increase $\gamma\gamma$ luminosity up to 10^{35}–10^{36} $\mathrm{cm}^{-2}\,\mathrm{s}^{-1}$ is described.

[18] V. I. Telnov, Nucl. Instrum. Methods Phys. Res. A **294**, 72 (1990).

[19] I. F. Ginzburg, in *Physics at LEP 200 and Beyond*, Proceedings of the Workshop on Elementary Particle Physics, Teupitz, Germany, 1994, edited by T. Riemann and J. Blumlein [Nucl. Phys. B (Proc. Suppl.) **37B**, 303 (1994)].

[20] Proceedings of the 10th Workshop on Photon-Photon Collisions, Photon '95, Sheffield, 1995 (World Scientific, River Edge, NJ, 1995).

[21] V. I. Telnov, Nucl. Instrum. Methods Phys. Res. A **355**, 3 (1995); V. E. Balakin and N. A. Solyak, *ibid.* **355**, 142 (1995); V. E. Balakin and A. A. Sery, *ibid.* **355**, 157 (1995).

[22] T. Maruyama *et al.*, Phys. Rev. Lett. **66**, 2351 (1991); T. Omori *et al.*, in *Proceedings of the High Energy Accelerator Conference*, Hamburg, 1992 (World Scientific, Singapore, 1992), Vol. I, p. 157; H. Aoyagi *et al.*, Phys. Lett. A **167**, 415 (1992); Y. Kurihara *et al.*, Jpn. J. Appl. Phys. **34**, 355 (1995).

[23] For a helical undulator method, see V. E. Balakin and A. A. Mikhailichenko, Report No. INP 79-85, 1979 (unpublished); K. Flöttmann, DESY Report No. DESY 93-161, 1993 (unpublished). For the other methods, see T. Okagi *et al.*, Jpn. J. Appl. Phys. 1 **35**, 3677 (1996).

[24] V. A. Ilyin *et al.*, KEK Report No. KEK-CP-030, 95-78 (unpublished); INP MSU Report. No. 95-16/380 (unpublished); Report No. hep-ph/9506326 (unpublished).
[25] E. Chopin, presented at the Proceedings of the 2nd European Workshop on Physics with e^+e^- Linear Colliders [13]; F. Boudjema and E. Chopin, Report No. ENSLAPP-A-534/95 (unpublished); Report No. hep-ph/9507396 (unpublished).
[26] An analogous procedure was used in [27] so as to see the contribution of higher-order monomials for heavy Higgs boson ($M_H \sim 1$ TeV and more).
[27] J. J. van der Bij, Nucl. Phys. **B267**, 557 (1986).
[28] E. E. Boos *et al.*, INP MSU/SNUTP Report No. INP MSU-94-36/358, SNUTP 94-116, 1994 (unpublished); Report No. hep-ph/9503280 (unpublished).
[29] G. J. Gounaris, D. Schildknecht, and F. M. Renard, Phys. Lett. **B83**, 191 (1979).
[30] V. Barger and T. Han, Mod. Phys. Lett. A **5**, 667 (1990).
[31] GRACE Manual, Vol. 1.0, KEK Report No. 92-19, 1993 (unpublished).
[32] E. E. Boos *et al.*, Int. J. Mod. Phys. C **5**, 615 (1994).
[33] K. J. F. Gaemers and F. Hoogeveen, Z. Phys. C **26**, 249 (1984).
[34] G. V. Jikia and Yu.F Pigorov, Phys. Lett. B **283**, 135 (1992).
[35] G. Jikia and A. Tkabladze, in Proceedings of the Workshop e^+e^- Collisions at 500 GeV: The Physics Potential, edited by P. W. Zerwas [DESY Report No. DESY 93-123C, 1993 (unpublished), p. 529]; G. V. Jikia, Nucl. Phys. **B412**, 57 (1994).
[36] N. Brown, Z. Phys. C **49**, 657 (1991); ''JLCI,'' KEK Report No. 92-16, 1992 (unpublished), p. 86; P. Grosse-Wiesmann, D. Haidt, and J. Schreiber, in Proceedings of the Workshop e^+e^- Collisions at 500 GeV: The Physics Potential, edited by P. W. Zerwas [DESY Report No. DESY 92-123A, 1992 (unpublished), p. 37].
[37] This value calculated by CompHEP and GRACE is in agreement with results obtained before by G. Jikia, Nucl. Phys. **B437**, 520 (1995); K. Cheung, Phys. Rev. D **50**, 4290 (1994).
[38] Z. Kunszt and W. Stirling, Phys. Lett. B **242**, 502 (1990).